

Operational Experience at the S-DALINAC *

A. Richter

Institut für Kernphysik, TH-Darmstadt, Schlossgartenstrasse 9, D-64289 Darmstadt, Germany

Abstract

A report on the status, the operational experience and the future perspectives of the superconducting Darmstadt electron linear accelerator (S-DALINAC) - one of the pioneering superconducting electron accelerators - will be presented. The S-DALINAC is an S-Band cw recirculating machine with a maximum energy of 130 MeV. Acceleration of the 250 keV electron beam from the gun and a preacceleration tube is achieved by a $\beta=0.85$, 2-cell capture section - followed by a $\beta=1$, 5-cell and ten 20-cell cavities. Unloaded Q values of all twelve superconducting Niobium cavities presently range from $8 \cdot 10^8$ to $2 \cdot 10^9$, while all gradients exceed 5 MV/m, some cavities reach 10 MV/m. Besides being an R&D project itself the S-DALINAC has produced since commissioning some 11000 hours of beam time for an ambitious experimental program in nuclear and radiation physics. Electron beams variable in energy from 3 to 120 MeV with currents up to $60 \mu\text{A}$, an energy spread of $\pm 2.5 \cdot 10^{-4}$ and an emittance of $\epsilon_n = 2\pi \text{ mm mrad}$ are employed routinely. Lately, numerous new beam diagnostics stations have been installed using transition radiation to determine the transverse and longitudinal beam parameters. Recently, the electron bunch length was determined as 4 ps with a charge of 4 pC per bunch at 10 MHz repetition rate. The S-DALINAC is also the driver of a Free Electron Laser (FEL) in the near IR. After spontaneous emission has already been observed the demonstration of stimulated emission is soon expected.

1 INTRODUCTION

First attempts to use superconducting rf structures for particle acceleration were undertaken in the 60's at Stanford University[1] and at the Kernforschungszentrum Karlsruhe[2]. The extreme expectations from the new technology first had to be followed by a few experimental drawbacks before, after some years of development the first electron accelerators were generated at the University of Illinois[3] and at Stanford University[4] and before at Argonne National Laboratory the first superconducting booster[5] for heavy ions became operative. The S-DALINAC is historically the third superconducting electron linac. It produced its first beam[6] in 1987 and went into full operation[7, 8] by the end of 1990. A brief description of the general layout of the S-DALINAC in Sect.1 is

followed by more detailed information on the most important parts for acceleration, the superconducting cavities and rf couplers, in Sect.3. Peculiarities of the accelerator, the different time structures of the electron beam and the adjustable lengths of the recirculating beam transport systems are described in Sect.4 and 5, respectively, whereas Sect.6 deals with beam diagnostics making use of transition radiation phenomena.

2 S-DALINAC: OVERVIEW

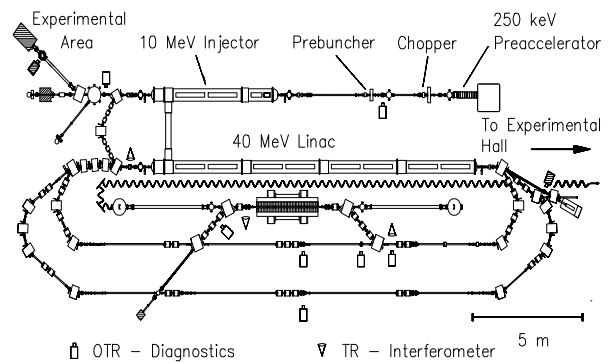


Figure 1: S-DALINAC with beam diagnostics stations.

The layout of the superconducting recirculating electron accelerator S-DALINAC as shown in Fig.1 above illustrates the principle of operation. The electron source is located on a high voltage terminal (top right) at 250 kV. The electrostatically preaccelerated beam gets its time structure (necessary for successive acceleration in the superconducting rf cavities at 3 GHz) in the chopper-prebuncher-section at room temperature, where the DC current from the source is first chopped into 30 ps long packages which are then bunched to a length of 5 ps when they enter the superconducting injector linac. Acceleration is then achieved by a 2-cell capture cavity ($\beta=0.85$) followed by a 5-cell capture cavity ($\beta=1$) and two 20-cell accelerating cavities, all fabricated from RRR=280 niobium and operated in liquid helium at 2 K. When leaving the injector, the beam has an energy of up to 10 MeV and can either be used for low energy experiments (photon scattering, investigation of channeling radiation (CR) and parametric X-rays (PXR)) or it can be bent isochronously by 180° for injection into the main linac. There, eight 20-cell cavities installed in four identical cryomodules increase the beam energy by up to 40 MeV. When

*Supported by BMBF under contract numbers 06 DA 655 I and 05 345 EAI 3 and through a Max-Planck Research Prize

leaving the main linac the beam can either be extracted to the experimental hall or it can be recirculated and reinjected one or two times by the appropriate beam transport systems (lower part of Fig.1). The maximum beam energy after three passes through the main linac therefore amounts to 130 MeV. The central part of Fig.1 shows the arrangement of the FEL[9]. There the beam from the straight section of the first recirculation is bent over and passed through the undulator and then either dumped or reinjected into the first recirculation for energy recovery experiments. Two mirrors to the left and right of the undulator form the 15 m long optical cavity and the wavy line in Fig.1 indicates the evacuated 50 m long transport tube for the radiation generated in the optical cavity. The symbols along the beam transport system mark locations of diagnostic stations described in Sect.6 below.

3 ACCELERATING CAVITIES AND RF-COUPLERS

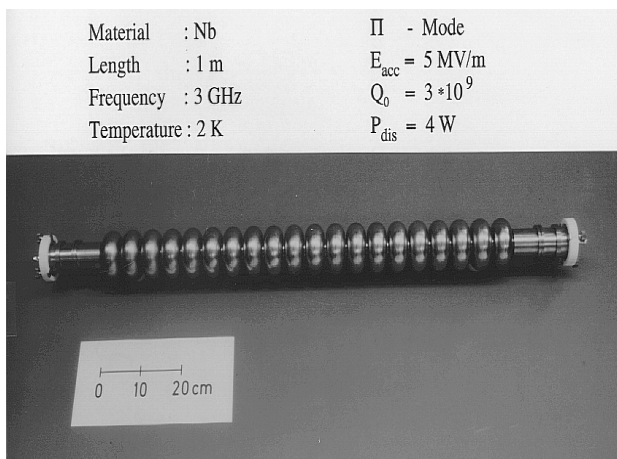


Figure 2: 20-cell 3 GHz superconducting cavity.

One of the superconducting 20-cell cavities of the S-DALINAC is displayed in Fig.2 together with its most important parameters. All cavities clearly exceed the design gradient of 5 MV/m, averaging $\langle E_{acc} \rangle = 6.7 \text{ MV/m}$. The only presently remaining drawback is the fact that the unloaded quality factors Q_0 are clearly lower than the expected value of $3 \cdot 10^9$, $\langle Q_0 \rangle = 7.7 \cdot 10^8$, resulting in increased dissipated rf power at 2 K. Since the helium refrigerator of the entire accelerator has only a capacity of 100 W at 2 K it is the dissipated rf power which has up to now limited the maximum beam energy to 120 MeV. We therefore continue to work on the improvement of Q_0 , the next measure in the very near future will be high pressure water rinsing of the inside of the cavities. The photograph of Fig.3 shows the youngest member of the S-DALINAC cavities, the 2-cell capture cavity with special rf couplers and its device for frequency tuning. Because of the reduced phase velocity ($\beta = 0.85$) the two cells are only 85 mm long. Nevertheless they increase the beam energy by 350 keV,

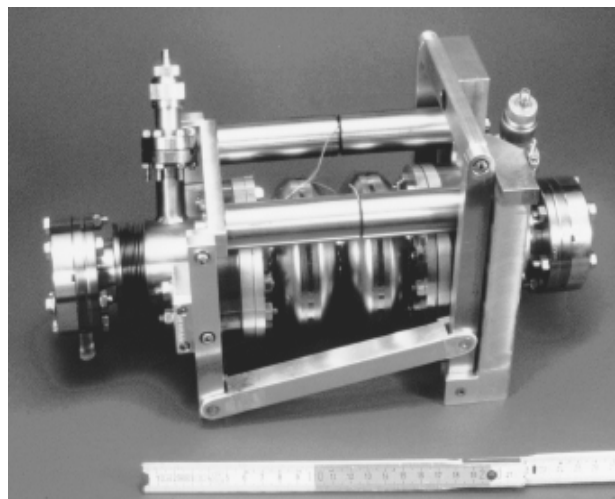


Figure 3: 2-cell capture cavity within its tuning frame.

when operated at a gradient of 5 MV/m, thus being equivalent to a rather powerful electrostatic preaccelerator. All

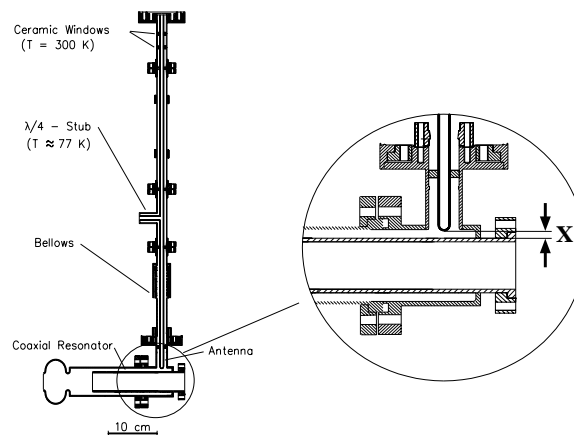


Figure 4: Layout of the tuneable sc input coupler.

the other accelerating cavities installed in the S-DALINAC are equipped with superconducting rf input couplers which provide variable coupling strength. The left part of Fig.4 shows the coupler together with its coaxial rf input line. The interior of this line is common with the beam vacuum and is therefore sealed with two ceramic windows at room temperature (the volume between the two windows is common to the insulating vacuum of the cryostat). Heat flow into the helium bath is minimized by the $\lambda/4$ -stub, which is thermally connected to a liquid nitrogen cooled reservoir at 77 K. Transfer of rf power from the input line to the cavity is performed in two steps: the coaxial line couples to the coaxial resonator (lower part of Fig.4) which in turn couples to the cavity (indicated by its first cell). Coupling between the coaxial line and resonator is determined by the distance x (right part of Fig.4) which can be varied by shifting the top part of the coaxial line vertically while keeping

the position of the coaxial resonator fixed (which is possible because of the bellows incorporated in the outer conductor of the coaxial line). The resulting variation in the overall

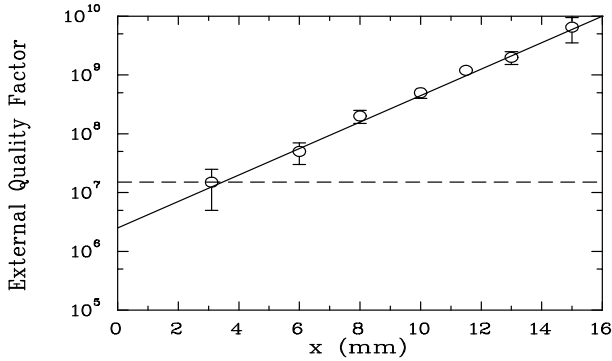


Figure 5: Demonstration of variable coupling strength.

coupling strength, expressed in terms of the external quality factor, is impressively shown in Fig.5 which displays a measurement at 2 K. It is quite obvious that not only different beam loading conditions can be matched ($Q_{ext} \approx$ a few 10^7), in situ diagnostic measurements at $Q_{ext} \approx 10^9$ are also possible with this coupler.

4 TIME STRUCTURE OF THE BEAM

In order to be able to drive the FEL installed at the S-DALINAC, the accelerator has to provide peak currents of 2.7 A. This could only be achieved by a reduction of the bunch repetition rate which has to be a subharmonic of the linac frequency. Therefore a pulsing option for the electron gun operating at a repetition rate of 10 MHz (300^{th} subharmonic) and a 600 MHz (5^{th} subharmonic) chopper/ prebuncher system had to be incorporated into the 250 keV injection of the accelerator. The central part of Fig.6 displays a schematic layout of the modified injection consisting from right to left of a 10 kV thermionic gun, a 250 kV electrostatic preaccelerator tube, a 3 GHz chopper/ prebuncher system for nuclear physics operation, a 600 MHz chopper/ prebuncher system for FEL operation, chopping aperture and the superconducting 2-cell and 5-cell capture sections. The upper and lower parts of Fig.6 show the time structure of the electron beam at the locations indicated by the arrows for the two modes of operation. For nuclear physics experiments, a continuous wave time structure with electrons in each rf bucket is produced. The chopper cavity together with the watercooled chopper aperture chops the DC current from the electron gun into pulses with a length of 30 ps. The prebuncher cavity compresses the width of these pulses to 5 ps at the entrance of the capture section of the superconducting injector linac. Since the beam is both accelerated and bunched in the capture sections the bunch length is further reduced to 2 ps at the end of the injector. For FEL operation the 1 ns wide pulses from the electron gun are chopped to a width of 370 ps by the 600 MHz subharmonic

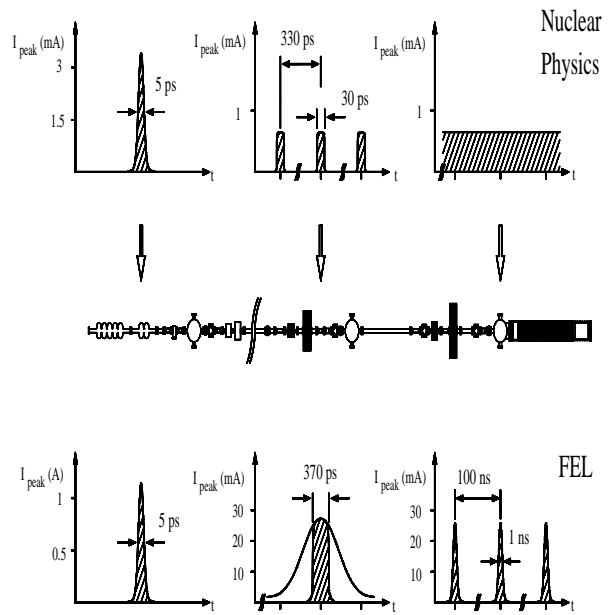


Figure 6: Time structure of the beam for 3 GHz cw (nuclear physics) and 10 MHz cw (FEL) mode of operation.

chopper and the chopper aperture. The subharmonic prebuncher then compresses the pulse width again to 5 ps at the entrance of the capture section. Similar to the 3 GHz continuous wave operation, the capture sections reduce the bunch length to 2 ps while increasing the peak current. Thus, the peak current corresponding to the emitted electron current of 27 mA from the gun amounts to 2.7 A.

5 BEAM TRANSPORT SYSTEM

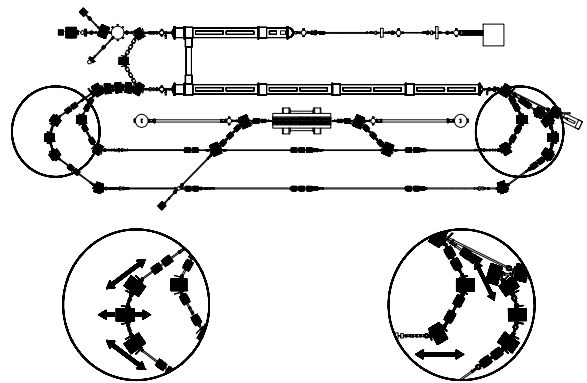


Figure 7: Pathlength adjustment for the recirculations.

In a low energy electron accelerator like the S-DALINAC the beam is not yet completely relativistic and therefore the time needed for a recirculation still depends slightly on energy. On the other hand at the entrance of the main linac the injection phase has to be the same for all three beams. It is thus necessary (since the accelerator has to provide a wide range of beam energies) to match the lengths of the recir-

culating beam transport system for each beam energy. The way this is done at the S-DALINAC is shown in Fig.7. The encircled parts of the layout (blown up in the insets) indicate where the path lengths adjustment is performed. In the first recirculation two dipole magnets and two quadrupoles are shifted on linear bearings in the direction of the arrows, allowing for a pathlength variation of $\Delta L = 50$ mm, corresponding to 180° of the rf phase. For the second recirculation (left inset in Fig.7) a length variation of $\Delta L = 62$ mm (220° of rf phase) is achieved by shifting three dipoles in the indicated directions.

6 BEAM DIAGNOSTICS

The location of new diagnostic stations along the accelerator is indicated in Fig.1 above and a detailed discussion of beam diagnostics at the S-DALINAC is given in[10]. Therefore only two examples for the determination of transverse and longitudinal beam properties using optical and far infrared transition radiation, respectively, are outlined here.

6.1 Transverse Phase Space

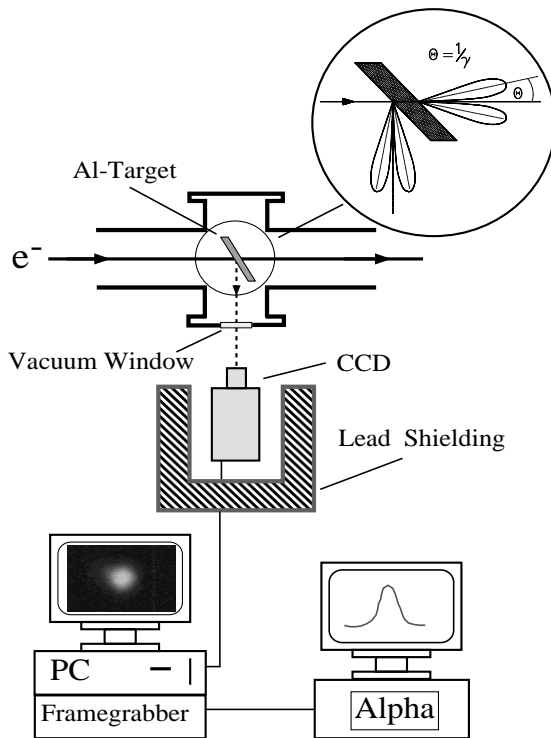


Figure 8: Schematic setup of an OTR diagnostics station.

The experimental setup for observation and analysis of optical transition radiation(OTR) is shown in Fig.8. The radiation produced by the electron beam hitting a $25\mu\text{m}$ thick aluminum target (the inset in Fig.8 shows the typical emission characteristics of OTR) is observed through a standard vacuum window by a well shielded CCD camera, whose

signals are digitized in a PC, equipped with a framegrabber board. Final analysis of the pictures is performed on a workstation using IDL[11] as dedicated software. OTR is used for diagnostic purposes at energies ranging from as low as 250 keV up to 120 MeV requiring a minimum beam current of $0.5 \mu\text{A}$ down to 10 nA, respectively.

6.2 Longitudinal Phase Space

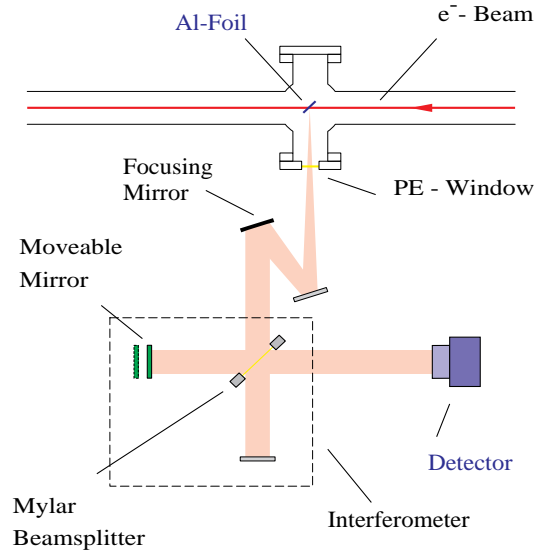


Figure 9: Autocorrelation setup for the transition radiation bunch length measurement.

For operation of the FEL, knowledge of the bunch length and thus the peak current is essential. The apparatus shown in Fig.9 makes use of the coherent far infrared part of transition radiation in the Michelson interferometer consisting of a mylar beamsplitter, a fixed and a moveable mirror, the radiation being detected by a pyroelectric detector. The result of the autocorrelation measurement is displayed in Fig.10 where the signal from the pyroelectric detector is plotted

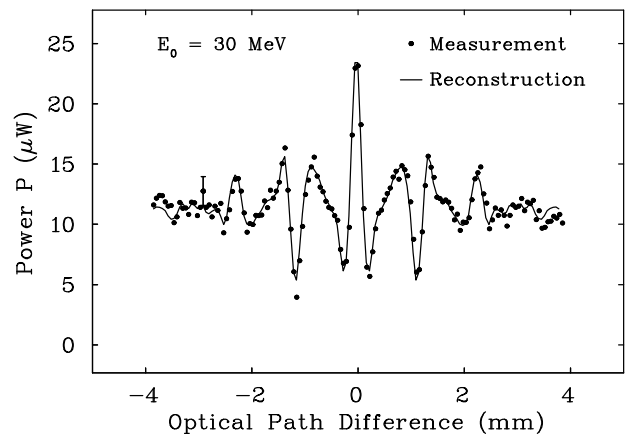


Figure 10: Autocorrelation measurement.

versus the position of the moveable mirror. A very elab-

orate analysis in frequency space(described in[12]) taking into account the spectral properties of the vacuum window, beam splitter and detector as well as water absorption finally yields a bunch width of 4 ps and a most likely shape as shown in Fig.11 where the result of this analysis is corroborated with a streak camera measurement using spontaneously emitted light from the undulator of the FEL.

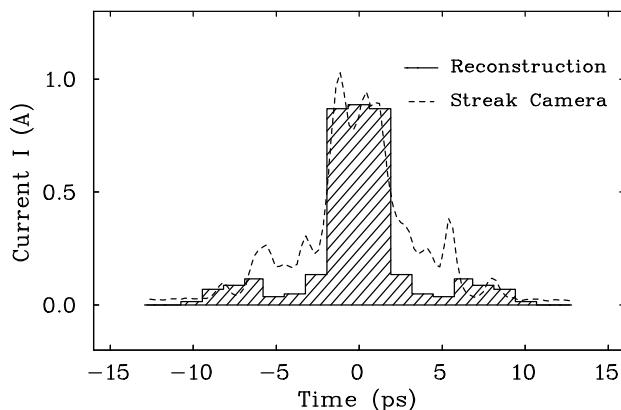


Figure 11: Puls shape measurements.

7 SUMMARY AND OUTLOOK

Since the end of 1990 when the S-DALINAC became fully operational it has produced more than 11000 hours of beamtime for different radiation and nuclear physics experiments (Nuclear Resonance Fluorescence (NRF) and inclusive (e,e') and exclusive ($e,e'x$) electron scattering) covering a very wide range of beam energies and currents as can be seen from the collection of operational data in Tab.1 below. For the near future we expect stimulated emission

Table 1: Characteristics of electron beams delivered to the experiments served by the S-DALINAC.

Experiment	Energy (MeV)	Current (μA)	Mode
NRF	2.5 - 10	40	3 GHz, cw
CR, PXR	3 - 10	0.01 - 10	3 GHz, cw
CR, PXR	85	1	3 GHz, cw
(e,e'), ($e,e'x$)	30 - 102	5	3 GHz, cw
FEL	30 - 38	$1.5 A_{peak}$	10 MHz, cw

from the FEL during its next beamtime scheduled for 1996. This optimistic assumption is based on several improvements achieved in the meantime. Diagnostics for all critical

beam parameters have been improved and new cavity mirrors with higher reflectivity and longer focal length, forming an optical cavity of higher Q and increased stability, are installed. The cavity length can now be determined by an interferometric measurement, thus narrowing the range where enough gain for stimulated emission can be expected. The accelerator will be operated in the 3 GHz cw mode routinely at energies up to 120 MeV. The two major improvements planned for the next year are: Installation of a high pressure water rinsing system for the cavities to improve on the unloaded quality factors and further optimization of the beam transport system which is expected to result in improved transverse stability properties by making use of non-isochronous recirculation. This will help to reduce the energy spread of the beam below the presently achieved value of $\pm 2.5 \cdot 10^{-4}$.

8 ACKNOWLEDGEMENT

The final design, construction, commissioning and current development of the S-DALINAC has been and is accomplished within the many diploma (47) and doctoral (19) theses of my students over the years. I am grateful to all of them as well as to my long term collaborators H. Genz, H.-D. Gräf, P.v. Neumann-Cosel, G. Schrieder, E. Spamer and O. Titze. The advice of I. Ben-Zvi, E. Haebel, H. Lengeler, H.A. Schwettman and T. Weiland at various stages of the project is appreciated. Also, much credit goes to the mechanical and electronic workshops not only of our institution but also of CERN and GSI. Finally, I thank particularly S. Döbert and H.-D. Gräf for their great help with the manuscript.

9 REFERENCES

- [1] J.M.Pierce, Proc. 9th Int. Conf. on Low Temp. Phys. A, Plenum, New York, (1965) 36.
- [2] A.Citron, Proc, Proton Lin. Acc. Conf., Batavia, FNAL, (1970) 239.
- [3] P.Axel et al., IEEE Trans. Ns-22 (1975) 1176.
- [4] C.M.Lyneis et al., IEEE Trans. Nucl. Sci. NS-28 (1981) 3445.
- [5] J.Aron et al., Proc. Lin. Acc. Conf., Ed. R.L. Witkover, BNL 511-34, Montauk, New York, (1979) 105.
- [6] J.Auerhammer et al., Proc. 5th Workshop on Rf Supercond., Ed. D.Proch, DESY M-92-01 (1992) 110.
- [7] V.Aab et al., Proc. 3rd Workshop on Rf Supercond., Ed. K.W.Shepard, ANL-Phy-88-1 (1988) 127.
- [8] J.Auerhammer et al., Nucl. Phys. A553 (1993) 841c.
- [9] H.Genz et al., Nucl. Instr. and Meth. A358 (1995) ABS20.
- [10] S.Döbert et al., Proc. EPAC 96, Barcelona (1996).
- [11] Interactive Data Language, Version 3.0, Research Systems (1993).
- [12] V.Schlott et al., Part. Accel. 52 (1996) 45.